

Compatibilizing effect of a maleic anhydride functionalized SEBS triblock elastomer through a reaction induced phase formation in the blends of polyamide6 and polycarbonate—III. Microscopic studies on the deformation mechanism

S. Horiuchi*, N. Matchariyakult, K. Yase and T. Kitano

National Institute of Materials and Chemical Research, 1-1, Higashi, Tsukuba, Ibaraki, Japan

and H. K. Choi and Y. M. Lee

National Institute of Technology and Quality, 2, Joogang-Dong, Kwachun, Kyungi-Do, Republic of Korea

(Received 13 January 1997)

Microscopic studies on the deformation mechanism of the blends of polyamide6 (PA6) and polycarbonate (PC) compatibilized with triblock copolymer of poly[styrene-*b*-(ethylene-*co*-butylene)-*b*-styrene] (SEBS) functionalized with maleic anhydride (SEBSgMA) were carried out. As described in our previous paper, significant improvement of mechanical properties of this blend series can be achieved by the use of the combination of SEBSgMA and unmodified SEBS (unSEBS) as compatibilizers. Especially, when the composition of the blends of PA6/PC is 75/25 and the total amount of added SEBS is 20 phr, drastic enhancement of the impact strength and of the elongation at break in the tensile stress–strain tests can be achieved by varying the ratio of SEBSgMA to unSEBS. The encapsulation by SEBS on the PC domains gradually become incomplete as the increase of the ratio of unSEBS to SEBSgMA and then the mechanical properties can be maximized. We observed the deformed zone of the specimens loaded to the tensile stress–strain tests and to the Izod impact tests using transmission electron microscopy (TEM) in order to find out the origin of this enhancement of the mechanical properties. It has revealed that voids tend to be generated at the PA6/PC interface easily due to the incompleteness of the encapsulation achieved by the use of the combination of SEBSgMA and unSEBS, and thereby the local shear yielding of the matrix is promoted to dissipate the tensile and the impact energy. © 1997 Elsevier Science Ltd.

(Keywords: polyamide6; polycarbonate; blend)

INTRODUCTION

Polyamide6 (PA6) and polycarbonate (PC) have been known to be incompatible, and the simple blending of PA6 and PC results in significant reduction of mechanical properties¹. Although some efforts for the compatibilization of this blend system have been reported, significant improvement of mechanical properties had not been achieved. Montaudo *et al.* synthesized some PA6/PC block copolymers and evaluated them as compatibilizing agents for the PA6/PC blends². Akiyama *et al.* evaluated poly(allylate-*co*-maleic anhydride) as compatibilizers for the blends of polyamides/PC blends^{3,4}. In both cases, the decrease of the size of dispersed domains can be successfully achieved, but mechanical properties however cannot be improved sufficiently.

We have been investigating the compatibilizing effect of poly[styrene-*b*-(ethylene-*co*-butylene)-*b*-styrene] (SEBS)

functionalized with maleic anhydride (SEBSgMA) in the blends of PA6 and PC^{5,6}. The interesting aspect regarding morphological feature which have been found is that the *in-situ* interfacial reaction between PA6 and SEBSgMA during melt blending induces the encapsulation by SEBS on PC dispersed domains in the PA6 rich blends. When unmodified SEBS (unSEBS) is added to the PA6 rich blends, unSEBS and PC are stuck together as dispersed domains in the PA6 matrix. Incorporation of SEBSgMA instead of unSEBS changes the morphology drastically. SEBSgMA is finely dispersed in the PA6 matrix and, at the same time, SEBSgMA encapsulates the PC domains. Moreover, when both SEBSgMA and unSEBS are added together into the PA6/PC blends by varying the ratio of SEBSgMA to unSEBS, the encapsulation by SEBS on the PC domains is gradually incomplete as increase of the ratio of unSEBS. We speculate that this morphological changing regarding the formation of domains composed by SEBS and PC in the PA6 matrix stems from the reduction of the interfacial tension between PA6 and

* To whom correspondence should be addressed

† Permanent address: Technology and Environmental Service, Rama 6 Road, Bangkok 10400, Thailand

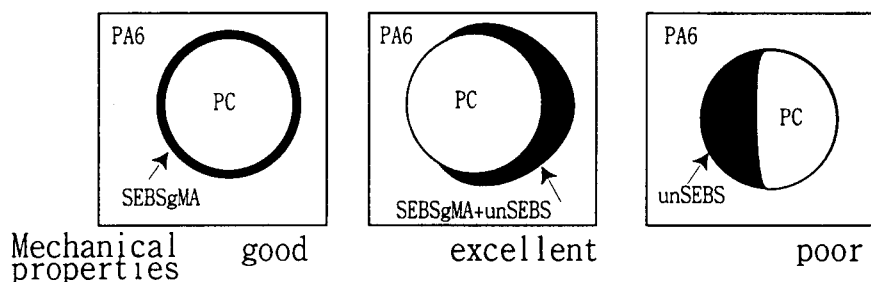


Figure 1 Schematic illustration for the formations of the domains composed by PC and SEBS obtained by varying the ratio of SEBSgMA to unSEBS in the blends where PA6 forms a matrix. The mechanical properties obtained through these formations as compared to the simple blends of PA6/PC are also indicated

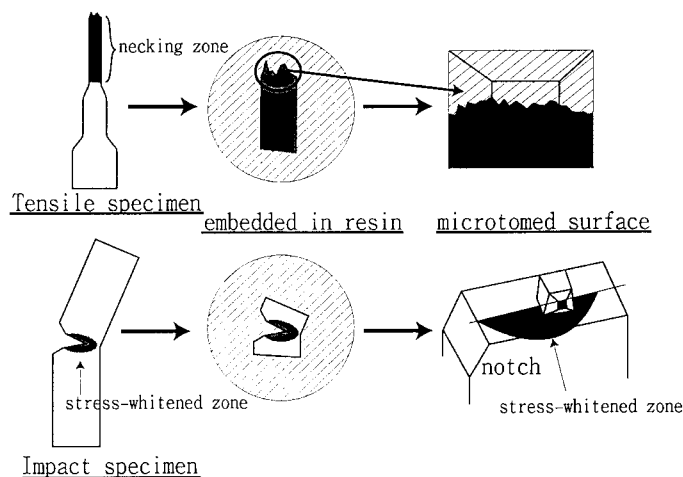


Figure 2 Procedure for the specimen preparation for TEM of tensile and Izod impact specimens

SEBS by the interfacial reaction^{5,7}. The Izod impact strength and the elongation at break in tensile stress-strain tests interestingly are maximized when the encapsulation is incomplete in both PA6 rich and PC rich blends⁶. *Figure 1* represents the phase formations of the domain composed by PC and SEBS in the PA6 matrix and the tendency of the mechanical properties obtained through these phase formations as compared to the simple blends of PA6/PC. Especially, when the total amount of added SEBS is held at 20 phr and the ratio of SEBSgMA to unSEBS is varied in the blends of PA6/PC 75/25 in weight ratio, drastic enhancement of the impact strength and of elongation at break in tensile stress-strain measurements have been achieved. As described in the previous paper⁶, the average size of the dispersed PC domains is almost constant when the ratio of SEBSgMA to unSEBS is varied and the interfacial situation between PA6 and PC is suggested to play an important role in this enhancement of the mechanical properties. In this paper, we carried out the microscopic studies in the deformed zone of the specimens using TEM to find out the origin of the toughness achieved by the use of the combination of SEBSgMA and unSEBS as compatibilizing agents for the blends of PA6 and PC.

EXPERIMENTAL

Materials and blending procedure

The base polymers used here are all commercially

available products. PA6 is supplied by Unichika (A1030BRF) with a number average molecular weight of 22 500 and melting flow rate of 4.3. The concentration of amine end group was determined at $5.0 \times 10^{-5} \text{ mol g}^{-1}$ by the titration. Bisphenol-A polycarbonate (PC) was supplied by Teijin Chemical (Panlite L-1250Y). The triblock copolymer, SEBS, supplied by Shell, is incorporated into the blends of PA6 and PC for compatibilizing of this system. This copolymer has styrene end blocks and a hydrogenated butadiene midblock resembling an ethylene/butylene copolymer. The SEBS functionalized with 2 wt% maleic anhydride onto the hydrocarbon chains of the mid block, which is designated SEBSgMA, is Kraton 1901. The molecular weight is 20 000 and the styrene content is 29 wt%. Unmodified SEBS is Kraton 1652 where molecular weight and styrene contents are the same as those of Kraton 1901.

Prior to processing, all polymers were dried at 80°C for at least 12 h in a vacuum oven to remove sorbed water. PA6 and PC were mixed using the compact mixer developed in our laboratory. The mixing part of this machine is illustrated in a previous paper⁵. A total of 10 g PA6 and PC with different amount of SEBSgMA and/or SEBS were put into the mixing chamber and were mixed at a rotation speed of 80 rpm at 260°C for 10 min. A blended sample was then pushed into a preheated mould placed just below the machine. The moulded sheet is 3 mm in thickness.

Analysis of the deformed zone

The notched Izod impact test and the tensile stress-strain test for these blends were carried out according to ASTM D256 and ASTM D638, respectively. The results were reported in our previous paper in detail⁶. In this work, we investigate the deformed zone of the specimens loaded to the impact and tensile tests using TEM. The procedure to view the morphology of the deformed zone is schematically summarized in *Figure 2*. First, fracture surface and opened crack are embedded in low shrinkage and low viscosity thermoset resin, Quetol 812, which is comprised of an epoxy resin and an anhydride as a curing agent, was used to prevent deformation during specimen preparation for TEM. The embedding resin was cured at 35°C of 7 days. Then, a small section of the specimen

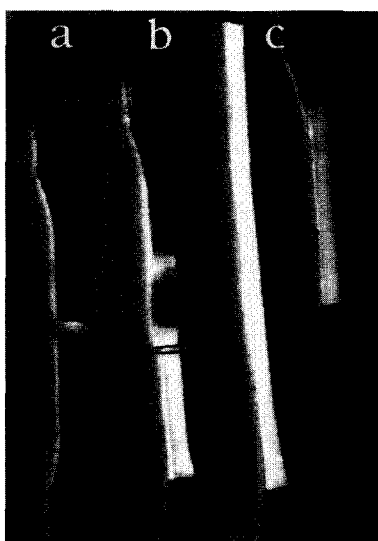


Figure 3 Tensile specimens showing three distinct fracture behaviours. (a) Tensile specimen of the simple blend of PA6/PC 75/25 showing brittle fracture. (b) Tensile specimen of the blend of PA6/PC/SEBSgMA 75/25/20 showing elongation at break of about 60%. (c) Tensile specimen of the blend of PA6/PC/SEBSgMA/unSEBS 75/25/10/10 showing the elongation at break of 235%

containing the fracture surface was cut out from the middle of the fracture plane by a diamond saw and then trimmed by a fresh razor blade to prepare the microtomed surface of area $0.2 \times 0.2 \text{ mm}^2$. Cryo-microtoming at -105°C was carried out with a diamond knife to prevent deformation during microtoming. The cutting direction is perpendicular to the fracture plane. The sections were of the order of $0.1 \mu\text{m}$ in thickness. Afterward the specimens were exposed to the vapour of 0.5 wt% aqueous solution of ruthenium tetroxide (RuO_4) for 10 min. RuO_4 stains both PC and the polystyrene (PS) blocks of SEBS. PS is relatively stronger stained than PC, hence the SEBS phase appears darker than the PC domains⁷.

TEM observation was carried out using a Zeiss CEM 902 at an accelerating voltage of 80 kV which attaches an integrated electron energy loss spectrometer to perform the energy-filtering TEM (EFTEM). The electron spectroscopic imaging (ESI) mode in EFTEM were applied to adjust the contrast of an image. The energy slit width is fixed at 20 eV and the energy loss level to be used was in the range 50–100 eV. Image recording and processing were performed using the Imaging Plate (IP) system, Fuji Photofilm FDL5000.

The measurements of density of the specimens were carried out to determine the volume dilation of the deformed zone. A gas displacement pycnometer, Shimadzu AccuPys 1330 was used.

To measure the area of the stress whitened zone in the Izod impact specimens, digital image analysis was carried out using NIH image software.

RESULTS AND DISCUSSION*Microscopic study on the deformation of tensile specimens*

Figure 3 shows the specimens exhibiting three distinct fracture behaviours in the tensile stress-strain tests. The simple blend of PA6/PC 75/25 failed in a brittle manner at strains less than 5% with no yielding. The specimens show no necking after the test (*Figure 3a*). On the other hand, the specimens of the blends of PA6/PC 75/25

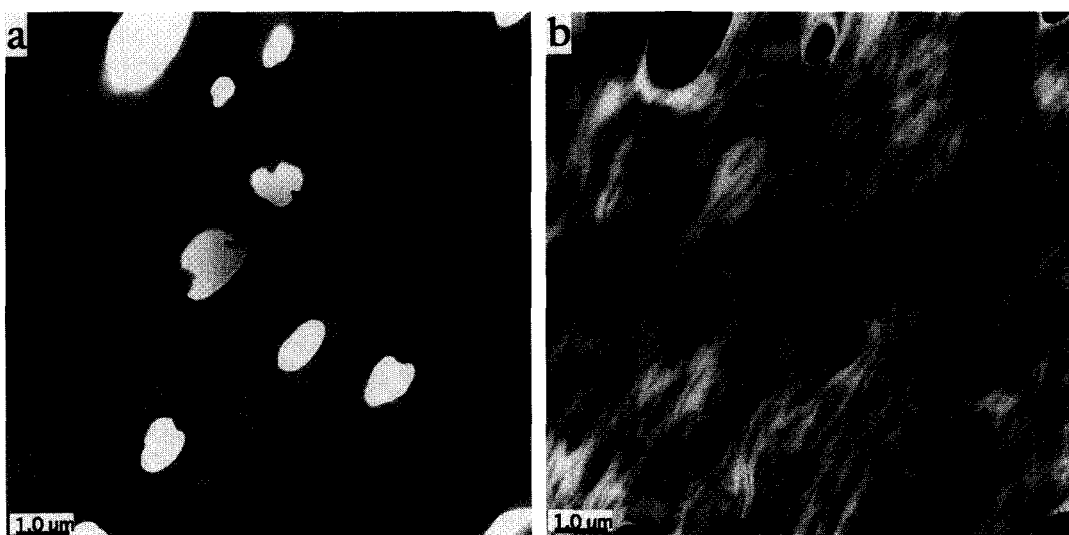


Figure 4 Two energy-filtering images taken by ESI mode in EFTEM at the same position of a specimen at different energy loss levels showing the deformed zone of the tensile specimen of the blend of PA6/PC/SEBSgMA/unSEBS 75/25/10/10. (a) Zero-loss image. (b) Energy-filtered image formed by electrons with an energy loss of $80 \pm 10 \text{ eV}$

compatibilized with SEBS-gMA failed by the succession of yielding, necking, necking propagation and final fracture. When 20 phr (20 g against 100 g of total amount of PA6 and PC) of SEBSgMA is added to the blend of PA6/PC 75/25, the specimens elongate at about 60% with necking before breakage (Figure 3b). When both unSEBS and SEBS-gMA were used together at certain ratios of unSEBS to SEBS-gMA, the elongation at break was drastically increased up to 250%. Figure 3c is the specimen of PA6/PC/SEBSgMA/unSEBS (75/25/10/10) exhibiting complete necking. We investigate the deformed zone of the tensile specimens using EFTEM in order to find out the origin of the drastic improvement of the elongation by the use of the combination of SEBSgMA and unSEBS.

Figure 4 shows the two energy-filtering images taken by ESI mode in EFTEM of the deformed zone just beneath the fracture surface of the blend of PA6/PC/SEBSgMA/unSEBS 75/25/10/10. These photographs were taken at the same position in a specimen in different energy loss levels. Figure 4a is a zero-loss image, which is imaged with unscattered and elastically scattered electrons passing through the specimen. The incident electrons pass through the voids without any interaction with the specimen, hence voids appear brighter than the other

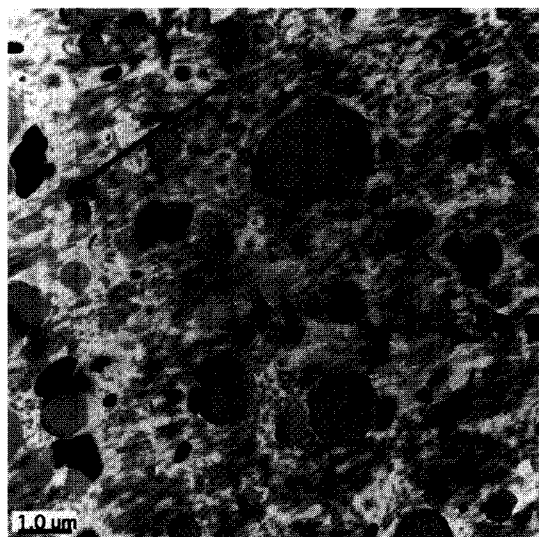


Figure 5 TEM photograph showing the deformed zone in the tensile specimen of the blend of PA6/PC/SEBSgMA 75/25/20. The arrow in the image indicates the direction of the deformation

area in an image. The zero-loss image cannot offer a clear image due to the large difference of brightness between the voids and the other areas. The energy-filtered image formed by electrons with an energy-loss of 80 ± 10 eV offers an image showing all regions in an image with an appropriate contrast (Figure 4b). No inelastically scattered electrons are generated from the voids in a specimen, hence the voids appear as the darkest area in an energy-filtered image formed by inelastically scattered electrons. Hereafter, we show energy-filtered images formed by inelastically scattered electrons for tuning the contrast of images.

As shown in Figure 4b, the deformed area contains many voids localizing at the PA6/PC interface in the blend of PA6/PC/SEBSgMA/unSEBS 75/25/10/10. The voids tend to exist at the front and/or the back sides of the PC domains and also tend to elongate into the tensile direction. Moreover, this photograph reveals the high deformation of SEBS domains dispersed in the PA6 matrix into thin domains oriented parallel to the tensile direction. Although the PC domains are somewhat deformed to be ellipsoidal in the tensile direction, the deformation of SEBS is much higher than that of the PC domains. On the other hand, in the blend of PA6/PC/SEBSgMA 75/25/20, the voids seem to be generated relatively uniformly throughout the PA6 matrix (Figure 5). Although some voids are located at the PA6/PC interface, the voids at the interface are not necessarily located at the front or the back side of the PC domains in the direction of the tensile deformation as observed in the blends of PA6/PC/SEBSgMA/unSEBS 75/25/10/10.

To estimate the void content in the necking part of the specimens, the volume dilation was determined by density measurements. Table 1 summarizes the volume dilation of the necking area of the specimens together with the elongation at break. The blends of PA6/PC with SEBS show significant increase of volume dilation after the tensile deformation, whereas the binary blends of PA6/SEBSgMA show lower volume dilation even after the long elongation at about 190%. In fact, the TEM photograph in Figure 6, showing the deformed zone of the binary blend of PA6/SEBSgMA 75/20, shows the higher deformation of SEBS domains into thin domains oriented parallel to the tensile direction, where neither cavitation of SEBS domains nor debonding of PA6/SEBS interface are identified, indicating that deformation is primarily by the shear yielding of the PA6 matrix. The interfacial adhesion between PA6 and SEBSgMA is strong due to the chemical reaction between them, hence

Table 1 Density of necking zone and the volume dilation in the tensile specimens and the elongation at break in tensile stress-strain tests

Sample	Density before the deformation (g cm^{-3})	Density after the deformation (g cm^{-3})	Volume dilation of stress whitened zone (%)	Elongation at break (%)
PA6/PC/SEBSgMA/unSEBS				
75/25/20/0	1.091	0.750	45.5	59.1
75/25/15/5	1.093	0.746	46.4	250.0
75/25/10/10	1.090	0.788	38.3	235.1
75/25/5/15	1.090	0.795	37.1	242.7
PA6/SEBSgMA				
75/20	1.056	0.975	8.4	182.9
75/10	1.097	0.994	10.4	200.0

the SEBS domains elongated into thin domains accompanying the shear yielding of the PA6 matrix. It has generally been known that deformation by dilational processes involves mainly crazing, rubber cavitation, voiding or debonding in the post-yield elongation. In the blends of both PA6/PC/SEBSgMA and PA6/PC/SEBSgMA/unSEBS, neither crazing nor rubber cavitation are observed in the deformed zone of the tensile specimens, thus the voiding and/or debonding are expected to occur primarily during the deformation. The observation of deformed zone and the measurements of the volume dilation indicate that the primary deformation in the blends of PA6/PC/SEBS is the shear yielding of the PA6 matrix accompanying the formation of voids or debonding at the PA6/PC interface which relieve the applied tensile stress. Although the volume dilation of the necking parts in the blend series of PA6/PC/SEBS are comparable, the elongation at break results in difference between the blend compatibilized with SEBSgMA alone and the blends compatibilized with both SEBSgMA and unSEBS. The difference of the elongation between these blend series may stem from the location of the voids generated during the tensile deformation. As shown in *Figure 4b*, SEBS located at the PA6/PC interface are highly elongated into the direction parallel to the tensile stress in the blends compatibilized with the combination of SEBSgMA and unSEBS. This suggests that the tensile energy can be dissipated by the deformation of the SEBS elastomer at the PA6/PC interface. As mentioned in our previous paper⁶, the SEBS phase existing at the PA6/PC interface tends to thicken as the ratio of unSEBS is increased. The thick SEBS phase on the interface exhibited the micro domain structure where the PS domains were arranged hexagonally in the poly(ethylene-butylene) (PEB) matrix. Through this formation, SEBS is expected to perform as an elastomer at the interface. Due to the imperfection of the encapsulation of SEBS on the PC domains to be achieved by the use of the combination of SEBSgMA and unSEBS, the debonding of the PC domains from the PA6 matrix may tend to occur easily at the interface where SEBS is not placed. The debonding is developed to a void by following applied tensile stress. The voids

however cannot be enlarged due to the energy dissipation by the deformation of SEBS located at the interface, hence the PC domains can endure to delaminate extensively from the matrix. In other words, the PA6/PC interface can be toughened owing to the performance of SEBS elastomer to prevent the delamination of the PC domains from the matrix. On the other hand, in the blends of PA6/PC with SEBSgMA alone, the encapsulation by SEBS on the PC domains is so perfect that the interfacial adhesion between PA6 and PC is assumed to be strong. Paul *et al.* reported the deformation mechanism of the blends of PA6 and polypropylene (PP) compatibilized with SEBSgMA⁸. In this case, SEBSgMA encapsulates the PP domains leading to great enhancement of mechanical properties. The deformed zone of the blends show the elongation of PP domains into thin domains in the PA6 matrix due to the strong interfacial adhesion⁹. On the contrary, in the blends of PA6/PC compatibilized with SEBSgMA, PC domains encapsulated by SEBSgMA show no such deformation as observed in the blends of PA6/PP compatibilized with SEBSgMA. This is because the stress necessary for the yielding of the PC domains is higher than the interfacial adhesion between PA6/PC and the yield stress of the matrix composed of PA6 and SEBS. Therefore debonding of the PA6/PC interface occurs before the yielding of the PC domains. In the blends of PA6/PC with SEBSgMA alone the SEBS phase on the PA6/PC interface shows no original micro domain structure since the SEBS phase at the interface is thin. Therefore, it is not expected to show the original performance as an elastomer. Once a void is generated at the interface, the SEBSgMA phase displacing at the interface between PA6 and PC cannot dissipate sufficient tensile energy, and the debonding leads to the delamination of the PC domain from the PA6 matrix. In fact, the deformation of SEBS locating at the PA6/PC interface is not identified in the blend of PA6/PC/SEBSgMA/unSEBS 75/25/20 (*Figure 5*).

Figure 7 shows the plots of the tensile yield stress as a function of the ratio of unSEBS to SEBSgMA together with the plots of the elongation at break in the blend of PA6/PC 75/25 with SEBS where the total amount of

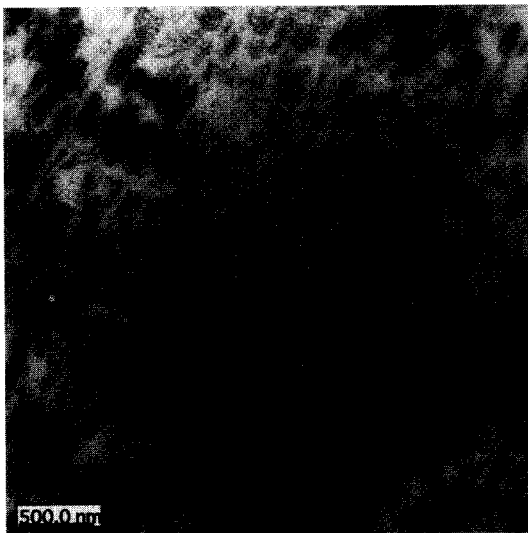


Figure 6 TEM photograph showing the deformed zone in the tensile specimen of the blend of PA6/SEBSgMA 75/20

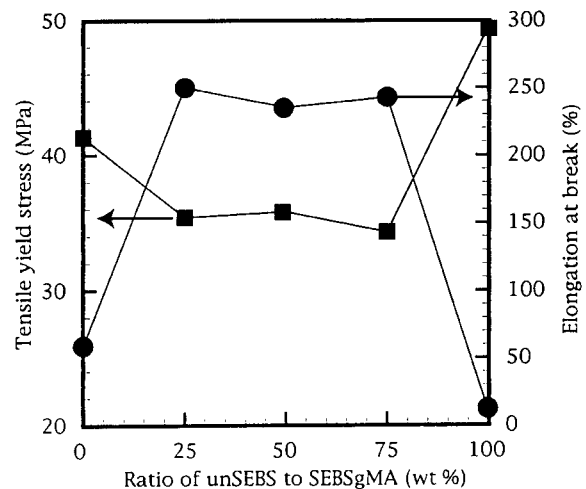


Figure 7 Tensile yield stress and elongation at break in the blends of PA6/PC/SEBSgMA/unSEBS as a function of the ratio of unSEBS to SEBSgMA. The composition of PA6/PC is 75/25 and the total amount of added SEBS is held at 20 phr

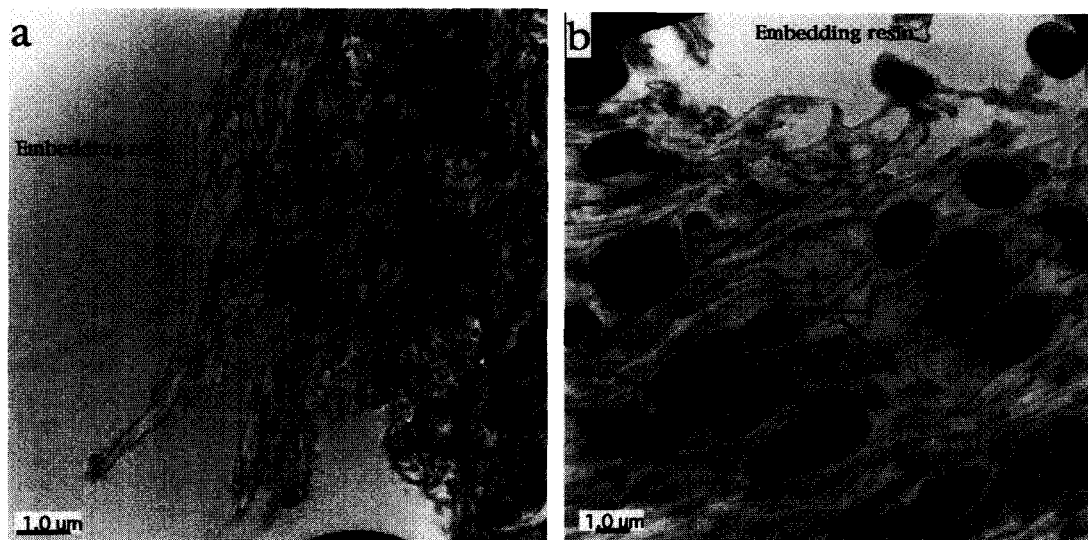


Figure 8 TEM photographs showing the deformed zone just beneath the fracture surface in the tensile specimens of the blends of (a) PA6/PC/SEBSgMA 75/25/10 and of (b) PA6/PC/SEBSgMA/unSEBS 75/25/10/10. The arrows indicate the deformed PC domains and the tensile direction

SEBS is held at 20 phr. This figure indicates that the tensile yield stress decreases when both SEBSgMA and unSEBS are incorporated together leading to the increase of the elongation. This implies that the voids are generated in the earlier stage of the strain in the blends of PA6/PC compatibilized with the combination of SEBSgMA and unSEBS rather than in the blend compatibilized with SEBSgMA alone. When both SEBSgMA and unSEBS are incorporated together in the blend of PA6/PC 75/25, debonding occurs at the earlier stage in the strain at the PA6/PC interface where SEBS is not located. Then, the debonding is developed into voids during the post-yield elongation. This is followed by extensive local shear yielding of the matrix around the voids accompanying the deformation of SEBS and then the tensile stress is relieved. As a result, the materials become ductile to achieve the great enhancement of the elongation. On the other hand, in the blend of PA6/PC/SEBSgMA 75/25/20, the void formation is assumed to be initiated at a relatively later stage of the strain due to the strong adhesion between PA6 and PC but once the void is generated, it soon results in the fracture of the specimen.

Figure 8 shows the TEM photographs of the deformed zone including the fracture surface in the blends of PA6/PC/SEBSgMA/unSEBS 75/25/20/0 and 75/25/10/10. In both cases, no PC particles seem to be exposed on the fracture surface. This means that the fracture path runs within the matrix composed by PA6 and SEBS without dislodging any PC domains. In the blend of PA6/PC/SEBSgMA 75/25/20/0 (*Figure 8a*), the PC domains just beneath the fracture surface are deformed into ellipsoids but no voids are generated at the interface. On the contrary, the deformation of the PC domains just beneath the fracture surface in the blend of PA6/PC/SEBSgMA/unSEBS 75/25/10/10 is significantly high in the direction of the tensile deformation with voids located at the PA6/PC interface (*Figure 8b*).

The above results imply that the deformation process during the tensile stress-strain test is different between the blends compatibilized with SEBSgMA alone and compatibilized with the combination of SEBSgMA and unSEBS, where PA6 forms the matrix. In the blends compatibilized with a combination of SEBSgMA and

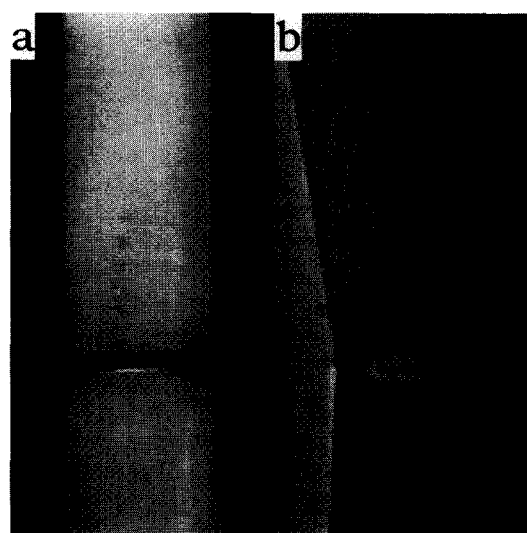


Figure 9 Side view around the notch of Izod impact specimens of brittle and tough specimens. (a) The blend of PA6/PC/SEBSgMA 75/25/10 showing no macroscopic stress-whitened zone. (b) The blend of PA6/PC/SEBSgMA/unSEBS 75/25/10/10 showing a stress-whitened zone surrounding the fracture plane

unSEBS, due to the imperfection of the encapsulation, debonding tends to occur at the PA6/PC interface easily at low strain level and then it can be arrested owing to the deformation of the SEBS phase located at the interface which results in the void formation at the interface. On the other hand, in the blends compatibilized with SEBSgMA alone, the perfect encapsulation by SEBS on the PC domains prevents the debonding of the PA6/PC interface and voids are generated at a later stage of the strain but it soon results in the fracture of the specimen. We suggest that the moderate imperfection of the encapsulation of SEBS on the PC domains is the origin of the significant enhancement of the elongation. This means that the void formation as a result of the debonding of the PA6/PC interface promotes the shear yielding of the matrix and thereby relieves the tensile stress.

Microscopic study on the deformation of Izod impact specimens

As for the results of tensile stress-strain tests, significant improvement of the Izod impact strength can be achieved when both SEBSgMA and unSEBS are added to the blends of PA6/PC 75/25, where the total amount of SEBS is held at 20 phr and the ratio is varied. When the ratios of SEBSgMA to unSEBS are between 19/1 to 5/15, the impact strength is higher than 550 J m^{-1} , while the strength is lower than 160 J m^{-1} in the other composition⁶. No intermediate values are obtained. This means that a sharp brittle-tough transition occurs when the ratio of SEBSgMA to unSEBS is varied. Figure 9 is the side view of the specimens of the blends of PA6/PC/SEBSgMA/unSEBS 75/25/20/0 and 75/25/10/10 after Izod impact tests. The Izod impact strength of the former is 154.1 J m^{-1} , while the latter is 640.3 J m^{-1} . In the tough specimens, the fracture is arrested and a stress-whitened

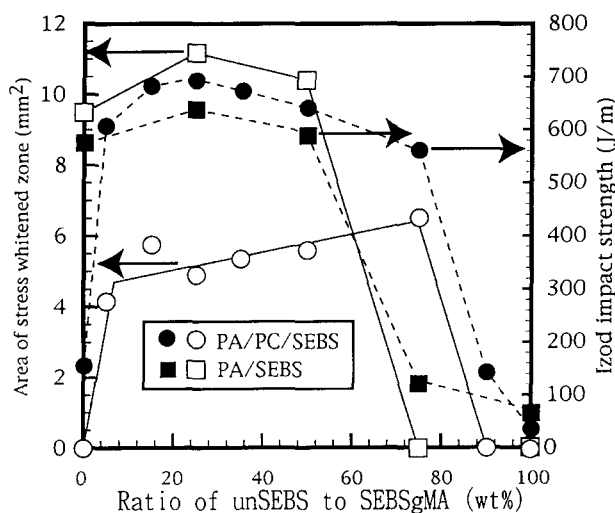


Figure 10 Area of stress-whitened zone and the Izod impact strength as a function of the ratio of unSEBS to SEBSgMA in the two blend series of PA6/PC/SEBS 75/25/20 and PA6/SEBS 75/20. The ratio of PA6 to SEBS is held at 75/20 in both blend series and the ratio of SEBSgMA to unSEBS is varied

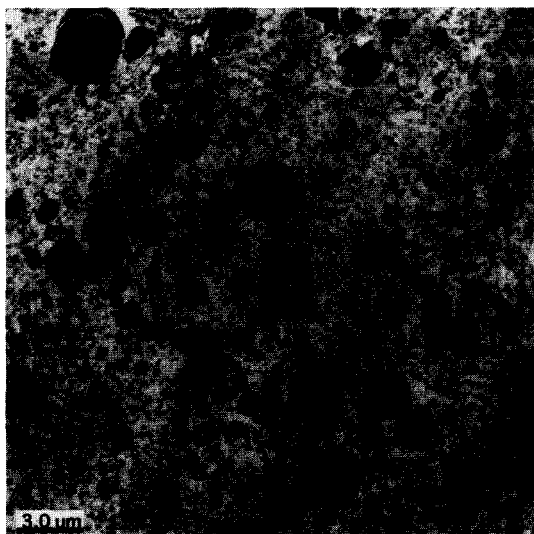


Figure 11 TEM photograph showing the stress whitened zone in the blend of PA6/SEBSgMA 75/20. The internal cavitation appears dark in the SEBS domains

zone is macroscopically observed to surround the impact fracture surface (Figure 9b), while in the brittle specimens, the fracture is complete and the stress-whitened zone is microscopic in size (Figure 9a). It has been recognized that the stress-whitened zone is the impact energy dissipation zone¹⁰. Moreover, the impact strength is increased with increase of the size of the energy dissipation zone. Figure 10 shows the area of the stress-whitened zone as a function of the ratio of SEBSgMA to unSEBS in the blends of PA6/PC/SEBSgMA/unSEBS and PA6/SEBSgMA/unSEBS where the ratio of PA6 to total amount of SEBS is held at 75/20 in both blend series. In this figure, the Izod impact strength is also plotted. The following can be noted from Figure 10: although the impact strength of tough specimens is of the same level in both blend series, the area of the stress-whitened zone of the blends of PA6/SEBS is approximately double that of the blends of PA6/PC/SEBS; the transition from brittle to ductile when the ratio of SEBSgMA to unSEBS is changed from 20/0 to 19/1 is unique to the blends of PA6/PC/SEBS; when the ratio of SEBSgMA to unSEBS is 5/15, the blend of PA6/PC/SEBS is still tough whereas the blend of PA6/SEBS is brittle.

To understand the above features in the relationship between the impact strength and the SEBSgMA/unSEBS ratio, we observed the stress-whitened zone of the specimens by TEM. First, the TEM photograph of the stress-whitened zone of the binary blend of PA6/SEBSgMA 75/20 is shown in Figure 11. This clearly shows the internal cavitation of the SEBS phase which indicates that the deformation mode in a high speed impact test is different from that in a slow tensile test. This result agrees with that reported by Paul *et al.* where they mentioned that SEBS rubber particles are able to cavitate under appropriate stress and high strain rate conditions⁹.

Figures 12a–c show the TEM photographs of the stress-whitened zone of the blends of PA6/PC/SEBSgMA/unSEBS 75/25/20/0, 75/25/19/1 and 75/25/5/15, respectively. In the blend of PA6/PC/SEBSgMA/unSEBS 75/25/20/0, the stress-whitened zone is microscopic in size, therefore the photograph of Figure 12a was taken just beneath the fracture surface near the notch. On the other hand, the photographs of Figure 12b and c were taken far from the crack front in the stress-whitened zone. All photographs reveal that the voids are generated primarily at the PA6/PC interface. It can be observed that the voids in the blend compatibilized with SEBSgMA alone is bigger and spreads on the PA6/PC interface more extensively rather than in the blends compatibilized with the combination of SEBSgMA and unSEBS. In the tough specimens, the degree of the void content and its size depends on the distance from the crack front in the stress-whitened zone, whereas in the brittle specimens, the voids can be observed only in narrow regions next to the fracture plane and the dependence on the distance from the fracture plane regarding the void size and content is not identified.

Figure 13 is a TEM photograph presenting a PC domain in a stress-whitened zone having a void at the interface in the blend of PA6/PC/SEBSgMA/unSEBS 75/25/19/1. A brighter zone surrounding the void can be identified. This indicates that the deformation of the matrix occurs locally at the interface around the voids. Moreover, the PC domain itself is found to be deformed

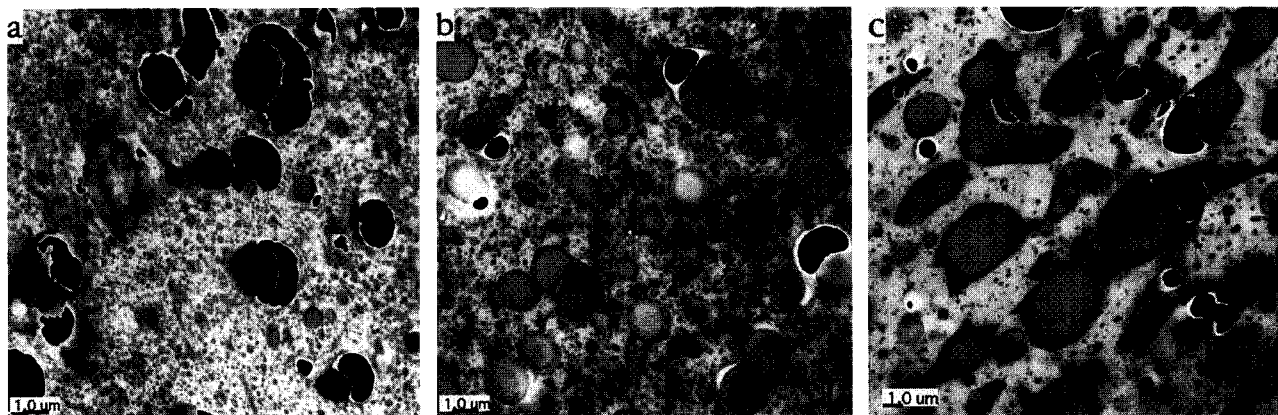


Figure 12 TEM photographs showing the stress-whitened zone in the blends of PA6/PC/SEBSgMA/unSEBS: (a) 75/25/20/0; (b) 75/25/19/1; (c) 75/25/5/15

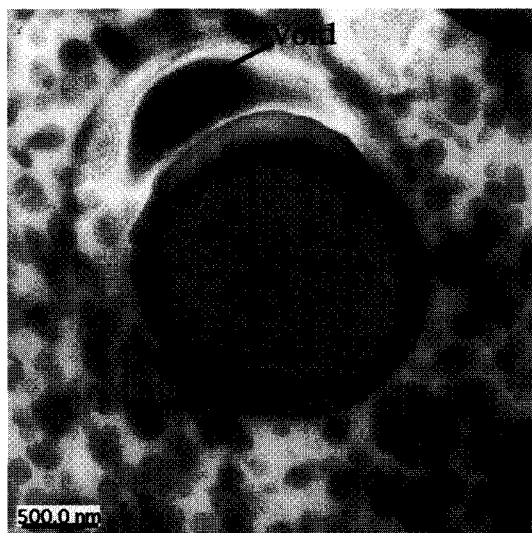


Figure 13 TEM photograph showing a PC domain in a stress-whitened zone with a void at the PA6/PC interface and with the deformation of PC near the interface in the blend of PA6/PC/SEBSgMA/unSEBS 75/25/19/1

near the PA6/PC interface. As discussed in our previous paper⁶, the average PC domain size is almost constant when the ratio of SEBSgMA to unSEBS is varied, while the SEBS domain size is increased as the ratio of unSEBS increase. Paul *et al.* reported that there is not only the upper limit size but also the lower limit size of the SEBS domain in terms of the impact strength in the PA6/SEBS blend series¹¹. However, the origin of the brittle-tough transition when the ratio of SEBSgMA to unSEBS is changed from 20/0 to 19/1 in the blends of PA6/PC 75/25 cannot be explained in terms of the dilation of the dispersed SEBS domain size because such a sharp transition is not detected in the blend series of PA6/SEBS with increase of the SEBS domain size. Therefore the difference of the interfacial situation between PA6 and PC is assumed to be the origin of the transition from brittle to tough. The observation of the stress-whitened zone suggests that the imperfection of the encapsulation by SEBS on the PC domains contributes to the void formation at the interface and then promotes the local deformation of the matrix. Wu has investigated the toughening mechanism of the PA6/rubber system to

show that the impact energy dissipation is achieved mostly by the yielding of the PA6 matrix¹². Also, Inoue *et al.* carried out an elastic-plastic analysis of the deformation in a PA/rubber system to reveal that the yielding of the matrix results in a large amount of energy dissipation, supporting the proposal by Wu¹³. The addition of rubber particles into the PA6 matrix causes voiding by internal cavitation of rubber particles or debonding at the PA6/rubber interface, which allows the local shear yielding of the matrix. This concept can be applied to the present case. As shown in *Figure 14a*, when SEBSgMA is used alone, the encapsulation is perfect. On the other hand, when the ratio of SEBSgMA/unSEBS is 19/1, the encapsulation by SEBS on the PC domain is slightly imperfect (*Figure 14b*). Due to the imperfection of the encapsulation in the blend of PA6/PC/SEBSgMA/unSEBS 75/25/19/1, debonding occurs predominantly at the PA6/PC interface with relatively low impact energy. But the SEBS rubber phase located at the interface prevents the debonding from spreading on the interface extensively through the energy dissipation by deformation of the SEBS rubber located next to the void. In the blend of PA6/PC/SEBSgMA/unSEBS 75/25/20/0, on the other hand, the encapsulation is so perfect that the higher energy is expected to be required to initiate the debonding. Once the debonding is initiated, however, it is easily developed to a large void extensively spreading on the PA6/PC interface without enough shear yielding of the matrix. The brittle-tough transition is thus assumed to stem from the difference in the interfacial situation between PA6/PC. In other word, toughness of the blends depends on the ability to produce the voids at the interface.

Although the tough specimens in both blend series of PA6/PC/SEBS and PA6/SEBS show comparable values of impact strength, deformation mechanism is different between them, as mentioned above. In the blends of PA6/SEBS, the internal cavitation of SEBS dispersed in the PA6 matrix is dominant, while in the blend of PA6/PC/SEBS, the debonding of the PA6/PC interface is dominant. Paul *et al.* have investigated the deformation mechanism leading to toughness in the compatibilized blends of PA6/PP⁹ and PA6/ABS¹⁴. They mentioned that cavitation of the rubber dispersed in the matrix and located at the interface is the important event followed by shear yielding of the matrix. In the present case, the debonding at the PA6/PC interface occurs primarily

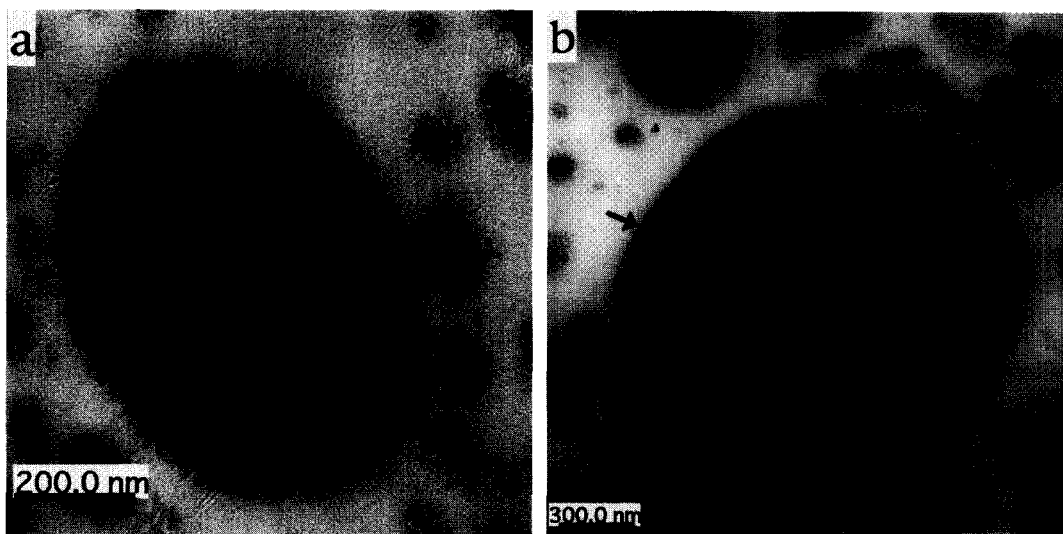


Figure 14 TEM photographs showing the encapsulation by SEBS on a PC domain in the blends of PA6/PC/SEBSgMA/unSEBS: (a) 75/25/10/0; (b) 75/25/19/1. The arrow in (b) indicates the place where the encapsulation is incomplete

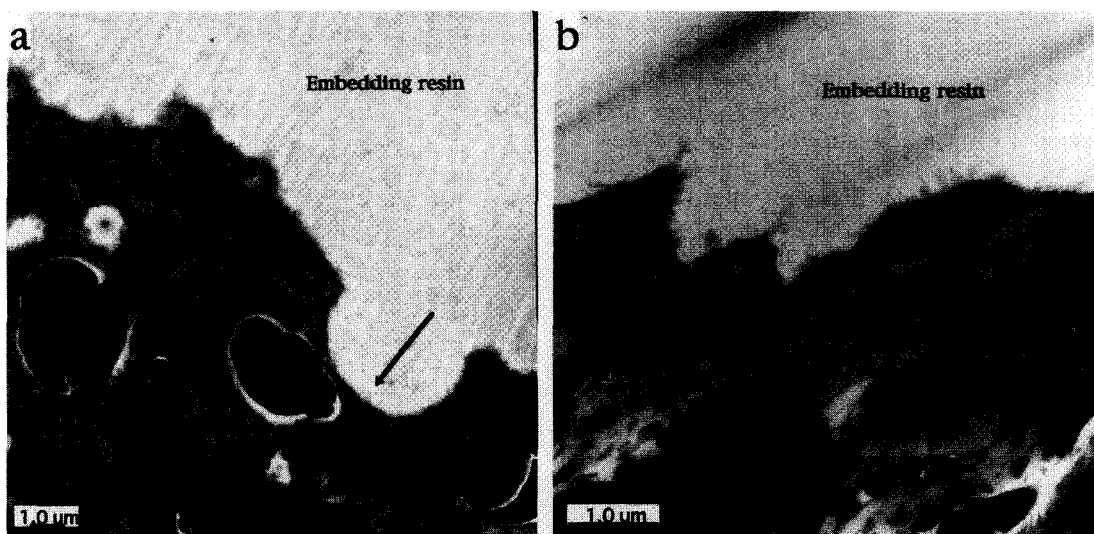


Figure 15 TEM photographs showing the fracture surface of the Izod specimens of the blends of PA6/PC/SEBSgMA/unSEBS: (a) 75/25/20/0; (b) 75/25/19/1. The arrow in (a) indicates the dislodging of a PC domain from the fracture surface

followed by the matrix yielding. This difference may be derived from the nature of the polymer. That is, PC has relatively high modulus and high yield strength as compared to PP and ABS. Thus, the PC domains are neither able to yield nor to create internal cavitation. As reported by Dompas *et al.*, debonding at the interface is as effective as internal cavitation with respect to the initiation of plastic deformation in the matrix in the blends of poly(vinyl chloride) (PVC) modified with methyl methacrylate-butadiene-styrene (MBS) copolymer¹⁵. Therefore, it can be mentioned that the moderate imperfection by SEBS on the PC domains causes the debonding at the PA6/PC interface and promotes the local shear yielding of the matrix which relieves the impact energy effectively.

When the ratio of SEBSgMA to unSEBS is 5/15, the blend of PA6/PC/SEBSgMA/unSEBS is still tough whereas the blend of PA6/SEBS is brittle (*Figure 10*). As described in our previous paper⁶, the blend of PA6/SEBSgMA/unSEBS 75/5/15 shows the bimodality in terms of the distribution of the SEBS domain size and the

average size is beyond the upper critical limit size. In the blend of PA6/PC/SEBSgMA/unSEBS 75/25/5/15, on the other hand, the voids are generated at the PA6/PC interface and the SEBS elastomer located at the interface is deformed (*Figure 12c*). Thus the void formation at the interface promotes the local shear yielding of the matrix and thereby the impact energy can be dissipated. On the contrary, in the blend of PA6/SEBSgMA/unSEBS 75/5/15, the cavitation is not expected to occur, showing that no stress-whitened zone is macroscopically observed, and thus resulting in brittleness.

As mentioned earlier, the area of stress-whitened zone in the tough specimens is much different between the blend series of PA6/SEBS and PA6/PC/SEBS although the impact strength shows comparable values. The area of the former is approximately double that of the latter. This difference stems from the difference of the voiding process in the two blend series. It can be inferred that the efficiency for the promotion of the shear yielding per void is higher in the blends of PA6/PC/SEBS than in the

blends of PA6/SEBS. Moreover, the deformation of PC domains as shown in *Figure 13* may contribute to the impact energy dissipation in the blends of PA6/PC/SEBS. The observation of the area just beneath the fracture surface offers clear evidence for the deformation of the PC domains (*Figure 15*). These two photographs show the deformed zone including the fracture surface in the blend of PA6/PC/SEBSgMA/unSEBS 75/25/20/0 and 75/25/19/1, respectively. In the blend of 75/25/20/0, the PC domains stay hemispherical and the dislodging of the PC domains from fracture surface is detected, indicating that the PC domains dislodge from matrix without significant deformation of the PC domains (*Figure 15a*). On the other hand, in the blend of 75/25/19/1, the PC domains are deformed into irregular shape with a void at the interface near the fracture surface (*Figure 15b*). The fracture surface seems to be smoother than that of the blend of 75/25/20/0.

CONCLUSIONS

In this paper, the mechanism for the significant improvement of the mechanical properties achieved in the PA6/PC 75/25 blends compatibilized with the combination of SEBSgMA and unSEBS has been explored. In the binary blends of PA6/SEBS, the deformation mechanism in the slow tensile mode and in the high speed impact mode is different. In the slow tensile mode, SEBS domains are yielded together with the matrix yielding, while in the high speed impact mode, the internal cavitation occur in the SEBS domains. On the other hand, in the blends of PA6/PC/SEBS where both SEBSgMA and unSEBS are incorporated together at certain ratios, it has been found that the void formation at the PA6/PC interface promotes the shear yielding of the matrix and leads to a significant increase of the elongation in the tensile test and also leads to the great enhancement of impact strength. The imperfection of the encapsulation by SEBS on the PC domains to be achieved by the use of the combination of SEBSgMA and unSEBS causes local debonding at the PA6/PC interface where SEBS is not located. But the debonding cannot spread on the PA6/PC interface rapidly by the deformation of SEBS rubber located at

the interface dissipating the applied tensile or impact energy. Thus voids are located at the PA6/PC interface in appropriate size and promote the local shear yielding of the matrix. In the PA6/PC 75/25 blends compatibilized SEBSgMA alone, the debonding cannot occur easily due to the perfect encapsulation by SEBS on the PC domains. However, once the debonding is initiated, it may rapidly propagate to the delamination of the PA6/PC interface and the subsequent local deformation of the matrix cannot occur sufficiently. This means that the strong adhesion is not sufficient for toughening. Through the compatibilization by SEBS in the blends of PA6/PC, the reduction of the PC domain size cannot be achieved as mentioned in our previous paper. Above all, the results suggest that the toughness of the interface is important in achieving high mechanical properties in incompatible polymer blends.

REFERENCES

1. Gattiglia, E., Turturro, A., Pedemonte, E. and Dondero, G., *J. Appl. Polym. Sci.*, 1990, **41**, 1411.
2. Montaudo, G., Puglisi, C., Samperi, F. and Lamantia, F. P., *J. Appl. Polym. Sci.*, 1996, **34**, 1283.
3. Sato, M., Akiyama, S. and Honda, S., *Kobunshi Ronbunshu*, 1990, **47**, 287.
4. Kim, Y. H., Akiyama, S. and Matusda, A., *Kobunshi Ronbunshu*, 1996, **53**, 169.
5. Horiuchi, S., Matchariyakul, N., Yase, K., Kitano, T., Choi, H. K. and Lee, Y. M., *Polymer*, 1996, **37**, 3065.
6. Horiuchi, S., Matchariyakul, N., Yase, K., Kitano, T., Choi, H. K. and Lee, Y. M., *Polymer*, 1997, **1**, 59.
7. Horiuchi, S., Matchariyakul, N., Yase, K. and Kitano, T., *Macromolecules* (in press).
8. Montiel, A. G., Keskkula, H. and Paul, D. R., *Polymer*, 1995, **36**, 4587.
9. Montiel, A. G., Keskkula, H. and Paul, D. R., *Polymer*, 1995, **36**, 4621.
10. Wu, S., *J. Polym. Sci., Polym. Phys. Ed.*, 1983, **21**, 699.
11. Oshinski, A. J., Keskkula, H. and Paul, D. R., *Polymer*, 1992, **33**, 268.
12. Wu, S., *Polymer*, 1985, **26**, 1855.
13. Fukui, T., Kikuchi, Y. and Inoue, T., *Polymer*, 1991, **32**, 2367.
14. Majumdar, B., Keskkula, N. and Paul, D. R., *J. Appl. Polym. Sci.*, 1994, **32**, 2127.
15. Dompas, D., Groeninckx, G., Isohara, M., Hasegawa, T. and Kadokura, M., *Polymer*, 1995, **36**, 437.